Conclusion

This chapter has been concerned with temporal and spatial variation in light intensity, and the effect of light on photosynthesis. The photosynthetic models have been limited to the aquatic environment, and confined to very simple equations. Models that are considerably more complex than those given here have been developed for these phenomena, principally to escape the limits of the assumptions of the simple models. Models of light are used in many simulations from biological fields other than those in this chapter. For example, light models are used in simulations of photosynthetic biochemistry, of plant and animal behavior cued by photoperiodism, and in visual phenomena. The relationship between solar radiation and temperature will be discussed in the next chapter.

CHAPTER 12

TEMPERATURE AND BIOLOGICAL ACTIVITY

Models of temperature are important in most fields of biological inquiry because of the effect temperature has on rates of biological activity. This is produced primarily by effects of temperature on chemical reaction rates. At low temperatures reaction rates become vanishingly small, and biological activity all but ceases. At high temperatures competing reactions, such as the denaturation of vital proteins are favored, and organisms begin to lose their integrity. Biological activity is primarily confined to temperatures between 0 and 100° Celsius. This chapter will describe some methods for modeling seasonal and daily variation of temperature and heat balance, and for describing the effect of temperature on rates of biological processes.

12.1 Seasonal and Daily Variation in Temperature

Temperature of the environment is largely a function of solar radiation. For this reason environmental temperatures tend to follow sinusoidal patterns like those of light intensity in the previous chapter. Temperature also partly depends on the quantity of heat stored in the environment as a result of solar inputs. If solar radiation were stored and reradiated uniformly, the temperature curve would be the integral of the solar sine curve. Analytically, the integral of a sine function is a negative cosine function:

$$\int \sin x \, dx = -\cos x + c \tag{12.1}$$

A negative cosine curve is identical to the sine curve, except that it lags the sine curve by 90° (i.e., it is out of phase by one-fourth wavelength). This relationship is diagrammed in Figure 12.1. The cosine approximation of temperature is inadequate, because the earth's surface is not homogeneous; air, land, and water can absorb, circulate and exchange heat energy at different rates. At most locations on the earth's surface, air temperature lags solar intensity by 3 to 4 weeks, rather than 13 weeks as

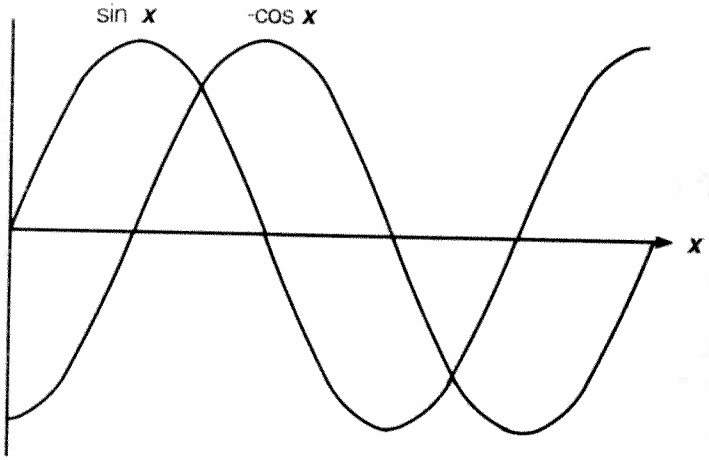

Figure 12.1. Comparison of sine curve with its integral, the negative cosine curve.

predicted by the negative cosine curve. If we use the 4-week figure and assume that average annual air temperature is 10°C with a range of 12°C for average daily temperatures on either side of the annual mean, we can find the average daily temperature for any week with

$$T = 10 + 12 \cdot \sin\left(2\pi \frac{W - 15}{52}\right) \tag{12.2}$$

This can be compared with a model for light intensity from Chapter 11:

$$I_d = 400 + 200 \cdot \sin\left(2\pi \frac{W - 11}{52}\right) \tag{12.3}$$

In many simulations, extremes of temperatures are more important than means. Webb et al. (1975) developed a model for air temperature of an Oregon forest which was composed of three elements: mean daily temperature, daily temperature range, and daily temperature excursion. Air temperature at any hour of any day is found with the relationship

$$\text{Air Temperature} = \text{Mean} + (\text{Range})(\text{Excursion}) \tag{12.4}$$

The following equations were used to find each of these components:

$$\text{Mean} = 10 + 8\sin\left(2\pi \frac{D - 107}{365}\right) \tag{12.5}$$

$$\text{Range} = 7 + 2\sin\left(2\pi \frac{D - 107}{365}\right) \tag{12.6}$$

$$\text{Excursion} = \sin\left(2\pi \frac{H - 17}{24}\right) \tag{12.7}$$

Equation 12.5 indicates that mean daily temperature has an annual average of 10°C, and a range of 8°C. This is multiplied by the sine function which starts its 365-day cycle on day 107 (17 April); the peak mean temperature of 18°C will come on day 198 (17 July). Equation 12.6 indicates that the average daily fluctuation of ±7°C in temperature will take place on days 107 and 290; the maximum fluctuation of ±9°C will occur on day 198. Equation 12.7 provides the timing of the daily temperature variation, with the minimum at 0400 (4 am) and a maximum at 1600 (4 pm). In these three equations, time is expressed as D, Julian calendar days, and as H, hours, from 0 to 24 with solar noon at 12.

Exercise 12-1: Write a program to simulate air temperature in an Oregon forest, using Equations 12.4-12.7. Perform time increments in nested FOR-NEXT loops, using the outer loop to increment days, and the inner loop for hours. Set up your program to produce graphical output showing air temperature for each hour during the weeks of 1-7 January and 4-10 July. Then modify your program to produce a graph of air temperature over the 24-hour period of your birthday. (This will be useful for planning your birthday picnic in an Oregon forest.)

12.2 Heat Balance in Biological Systems

Heat balance determines the temperature of natural objects and organisms. If an object is absorbing or generating heat faster than it is giving off heat, obviously its temperature must rise. In this section we will consider the heat balance of an entire lake, and also of a desert-dwelling mammal.

The major source of heat energy input for a lake is solar radiation striking its surface. It is not surprising that the heat content and water temperature of a lake will follow an approximate sine function on an annual basis. The energy budget equation which describes the heat content

of a lake is

$$Q_{t+\Delta t} = Q_t + (I_t + S_t - E_t - O_t) \tag{12.8}$$

where Q_t is the heat content of a lake at time t, and $Q_{t+\Delta t}$ is the heat content one week later. Heat content is measured on the basis of the exposed surface of the lake, as calories cm^{-2}. The other components of the equation are I_t, the effective radiation coming in through the lake's surface; S_t, the sensible heat transfer by conduction or convection to or from the atmosphere; E_t, the heat lost or gained by evaporation or condensation; and O_t, the heat lost as radiation to the atmosphere. These four components are rates, and are each expressed below as calories cm^{-2} $week^{-1}$.

Radiation input by weeks may be described by the following equation:

$$I_t = 2800 + 1400 \sin\left(2\pi \frac{w - 11}{52}\right) \tag{12.9}$$

The form of this equation and the constants have been described above (e.g. Equation 12.2). Sensible heat transfer is based on Newton's law of cooling (see Chapter 1) and is given by

$$S_t = k\,(T_a - T_w) \tag{12.10}$$

where T_w is the surface temperature of the water and T_a is the temperature of the air overlying the water. Air temperature may fluctuate as in Equation 12.2. The transfer coefficient will vary with wind velocity; you may assume that it has a value of 100 calories cm^{-2} $week^{-1}$ $°C^{-1}$

Evaporation removes heat from the lake and may be described by the equation

$$E_t = RH\,(P_w - P_a) \tag{12.11}$$

The various terms in this equation are defined as follows. R is a rate constant that depends on wind velocity. Assuming an average wind velocity of 10 m sec^{-1}, R will have an approximate value of 1.0 gram $mmHg^{-1}$ cm^{-2} $week^{-1}$. H is the latent heat of evaporation and is a function of water temperature. Over the range of 0 to 50°C, H may be approximated by this equation:

$$H = 595.8 - 0.54T_w \tag{12.12}$$

P_w is the saturation water vapor pressure, which is also a function of surface water temperature. P_w is approximated by a cubic equation (Chapter 3):

$$P_w = 4.57 + 0.357T_w + 0.0065T_w^2 + 0.0004T_w^3 \tag{12.13}$$

P_a is the partial pressure of water vapor in the air and is quite variable. For purposes of this simulation we may assume a constant 80 percent relative humidity, so that P_a will be a function of air temperature as follows:

$$P_a = 3.66 + 0.286T_a + 0.0052T_a^2 + 0.0003T_a^3 \tag{12.14}$$

According to the Stefan-Boltzmann law, thermal radiation of the lake to the atmosphere is a function of the absolute temperature of the lake surface, raised to the fourth power. The atmosphere will also radiate to the lake as a function of atmospheric temperature. The relationship between atmospheric temperature and radiation is not simple (Hutchinson 1957). We will employ a simple equation that relates the net thermal radiation between a lake and the atmosphere to the difference between air temperature and water temperature:

$$O_t = 77(T_w - T_a) \tag{12.15}$$

where O_t is the net thermal radiation with units of calories cm^{-2} $week^{-1}$.

Exercise 12-2: Prepare a flowchart for a program to simulate water temperature of a lake based on the heat-balance model described with Equations 12.8-12.15. Then implement your program using the given transfer coefficients and rate constants. The output of your program should consist of a graph showing lake temperature for 104 weeks (2 years). Assume the lake has an initial temperature of 6°C on January 1, and that the lake circulates continuously throughout the year. Also assume the lake to have an average depth of 10 meters, so that

$$(T_w)_t = \frac{Q_t}{1000} \tag{12.16}$$

based on the specific heat of water of 1 calorie $gram^{-1}$ $°C^{-1}$. Although this simulation appears complex because of the number of equations involved, it is in fact greatly simplified and ignores many important features of the lake environment, including stratification. Section 12.7 below describes a model that includes stratification. For more information on models of heat balance for lakes, see Hutchinson (1957) and Wetzel (1983).

Exercise 12-3: Like most mammals placed in a hot environment, camels regulate their body temperatures partially by evaporative cooling (sweating) if they have enough drinking water. However, a partly dehydrated and thirsty camel exposed to heat will conserve water, and rather than sweating will allow its body temperature to increase. This takes advantage of the decreased rate of transfer of

heat that occurs with increased body temperatures in warm environments (Newton's law). Camels rely on large body mass, about 460 Kg as an average, to moderate effects of increased heating. While the sun shines, a camel's body will absorb heat and increase in temperature, and during the relatively cool desert night it will lose heat.

Write a program to simulate the body temperature change of a partly dehydrated camel, based on the following considerations: (1) Internal metabolic heat production is constant at 250 Kcal hour^{-1}. (2) Air temperature varies sinusoidally on a 24-hour cycle, with a maximum of 46°C at 1400, and a daily mean of 33°C. (3) Between a camel's body and air, thermal conductance k is 62.5 kcal hour^{-1} °C^{-1}; heat loss and gain follow Newton's law (Equation 1.10; see also Equation 12.10). (4) T_t, body temperature at time t, is found with Q_t/M, where M is body mass in kilograms and Q_t is total heat content at time t.

Begin your simulation at midnight with a camel having a body heat content of 16500 kcal above 0°C. For each hour, find the total heat gained or lost by the camel (kcal), and plot the results of your simulation over a 96-hour period. Also produce a graph showing body temperature of the camel over the same time period.

12.3 Effect of Temperature on Chemical Reaction Rates

Biological activities such as feeding, digestion, respiration, photosynthesis, growth, and movement depend on chemical reactions which are catalyzed by enzyme proteins. Because of this dependency, temperature will affect biological activity in two ways. First, a temperature rise will increase the number of reactant molecules having an energy equal to or greater than the activation energy for the reaction. This effect tends to increase the reaction rate. Second, high temperatures may denature enzyme molecules, causing them to lose their catalytic activity. These two effects compete, resulting in the typical temperature optimum curve associated with essentially all biological activity. Some models of temperature dependency of biological systems are described in the next few sections.

One of the earliest models dealing with the effect of temperature on chemical reaction rates was developed by Arrhenius in 1889, based on the concept of activation energy. This equation defines the change in reaction rate with temperature as follows:

$$\frac{d(\ln k)}{dT} = \frac{(E_a)}{RT^2} \tag{12.17}$$

where k is the reaction rate constant, T is absolute temperature in °K, R is the gas law constant, and E_a is the activation energy for the reaction. When integrated analytically, this equation can take the following form:

$$\ln k = \left(\frac{-E_a}{r} \cdot \frac{1}{T}\right) + \ln k_\infty \tag{12.18}$$

where $\ln k_\infty$ is an integration constant, representing the limiting value of k.

Notice that this is an equation for a straight line. This allows $\ln k$ to be graphed as a function of $1/T$, and therefore to obtain $-E_a/R$ as the slope. These Arrhenius plots are often used to find the activation energy for various biological reactions.

By integrating Equation 12.18 between limits and taking antilogs, the equation becomes

$$k_T = k_x \exp\left(\frac{E_a}{R} \cdot \frac{(T - T_x)}{T \cdot T_x}\right) \tag{12.19}$$

where k_T is the rate at temperature T, and k_x is the rate at some reference temperature T_x . Equation 12.19 can be made more useful by expressing temperature as °C rather than °K. The reference temperature is set to 0°C, and E_a/R is combined as a single constant:

$$k_C = k_0 \exp\left(\frac{A \cdot C}{C + 273}\right) \tag{12.20}$$

In this form, k_C is the rate at some Celsius temperature C, and k_0 is the rate at 0°C. The value of the constant A may be found from the slope of the Arrhenius plot, where

$$A = \frac{\text{Arrhenius slope}}{273} \tag{12.21}$$

The value of A may also be estimated from the Q_{10} value (see below) and Equation 12.20. For further discussion of the development of the Arrhenius equation, see Hamil et al. (1966).

A simple and widely used method for describing the effect of temperature on chemical reactions is called the Q_{10} approximation. Q_{10} is the factor by which reaction velocity is increased for a temperature rise of 10°C. The equation, in a form like Equation 12.20, is

$$k_C = k_0 Q_{10}^{C/10} \tag{12.22}$$

or

$$k_2 = k_1 Q_{10}^{(C_2 - C_1)/10} \tag{12.23}$$

where k_2 and k_1 are rates at temperatures C_2 and C_1. The equation is useful over relatively narrow ranges of temperature. Prosser and Brown (1961) discuss this problem further.

12.4 Effect of Temperature on Enzyme Activity

The amount of product produced by a reaction catalyzed by an enzyme depends on two reactions that have different rates. One reaction is the actual formation of product; the other is the denaturation of the enzyme. These reactions may be written together as follows:

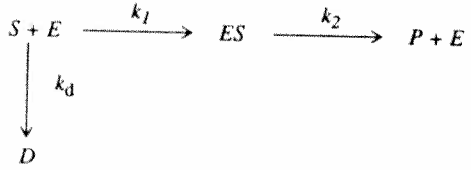

where E is the active form of the enzyme, D is the denatured form, P is the product, S is the substrate, and ES is the enzyme- substrate compound. The rate of product formation is

$$\frac{dP}{dt} = k_2[ES] \tag{12.24}$$

If substrate is in excess and k_2 is the rate constant for the limiting reaction, we may assume that ES is in equilibrium with E and S, so that k_1 is given by

$$k_1 = \frac{[ES]}{[E][S]} \tag{12.25}$$

If this equation is rearranged and substituted into Equation 12.24, then

$$\frac{dP}{dt} = (k_2 k_1[S])\,[E] = k_r[E] \tag{12.26}$$

where k_r is an overall constant involving k_1, k_2, and substrate concentration $[S]$, which will be essentially constant if in great excess. The reaction now simplifies to

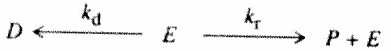

The effect of temperature on k_r may be modeled using a modification of Equation 12.20:

$$(k_r)_T = (k_r)_0 \exp\left(\frac{A_r T}{T + 273}\right) \tag{12.27}$$

where T indicates temperature in °C.

The denaturation rate constant, k_d, also depends on temperature, and may be described by an equation similar to 12.27. Because of the very high activation energy involved, the reaction has a very high value of A_d, which is equivalent to a very high Q_{10} value. Here we will assume that denaturation is controlled totally by kinetic effects. The equation would be much the same if instead we were to assume a temperature effect on the equilibrium constant involved in the denaturation reaction.

Exercise 12-4: Using the equations above, write a program to simulate the effect of temperature on an enzyme-catalyzed reaction. Base your measurement of rate of product formation (i.e. activity of enzyme) on amount of product that is obtained after the reaction has proceeded for some arbitrarily specified period of time. Because denaturation of the enzyme depends on time, the optimum temperature shown by your simulation will partly be a function of length of this time period, as shown in Figure 12.3. A flowchart for the program is shown in Figure 12.2. Implement your simulation using the following values:

$$(k_r)_0 = 1 \quad (k_d)_0 = 0.0001 \quad A_r = 18$$
$$A_d = 55 \quad E_0 = 2 \quad t_{\max} = 20$$

Set $\Delta t = 0.01$. The output of your simulation should be a graph of the amount of product vs. temperature, for temperatures from 0 to 80°C. Your graph should resemble a typical optimum temperature curve like those of Figure 12.3.

12.5 Models of Temperature Effects on Biological Activity

Many models have been published to describe effect of temperature on rates of biological processes. The available literature is so large that Watt (1975) described it as "truly awesome". Many of these models attempt to use simple enzyme effects for complex biological processes involving many enzymes. In general, such models assume that a single enzyme will limit rates in complex systems like a developing embryo or feeding animal. The response of the whole organism is assumed to be similar to that of the limiting enzyme. This assumption is usually incorrect, because different enzymes can be limiting at different temperatures.

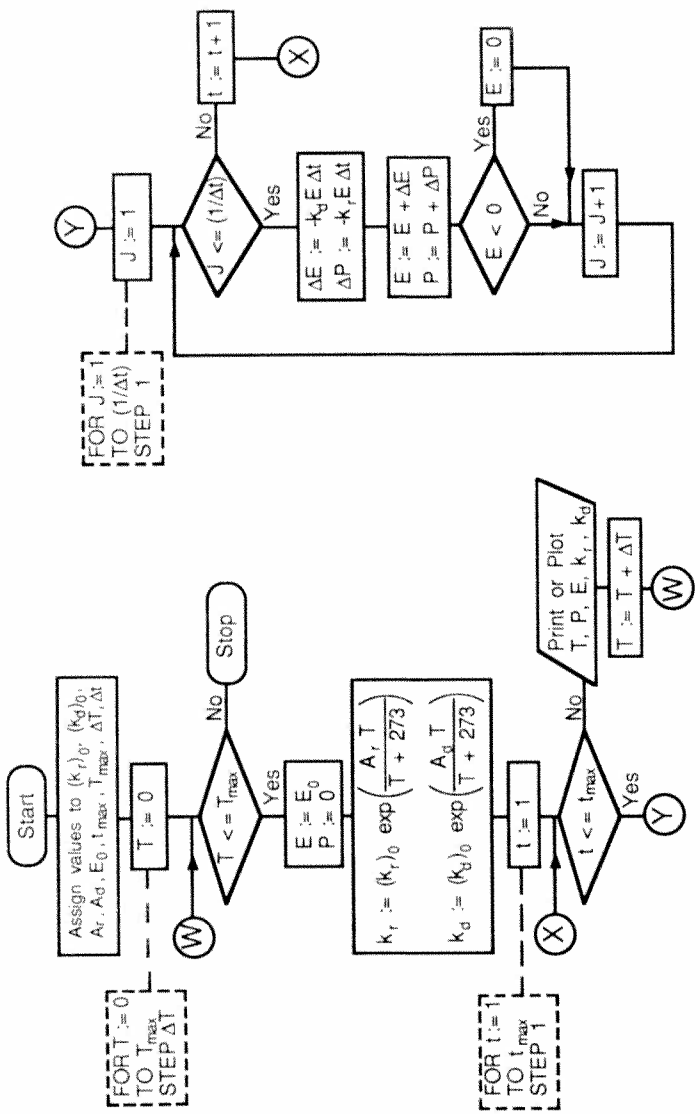

Figure 12.2. Flowchart for a program to simulate the effect of temperature on activity of enzymes.

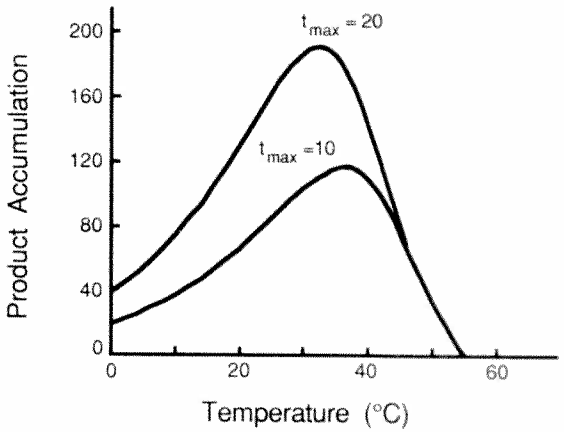

Figure 12.3. Curves showing simulation results of response of enzymes to different temperatures.

Overall response of a biological process to temperature is a composite of the response curves of all enzymes that might limit the rate within the temperature range for the organism. An overall response curve may be very different from that produced by a single enzyme. For example, Sharpe and DeMichele's (1977) model of development rate at different temperatures was based on Eyring's transition-state theory (Johnson et al. 1954, Eyring and Urry 1965). Assuming a single limiting enzyme, the model uses six constants that must be estimated from data. They note that the composite curve from multiple limiting enzymes could be described with their equation. The constants then would be simply regression coefficients for an empirical equation.

We present here two empirical equations which have been used to describe effects of temperature on biological rates. Below optimum temperature the rate rises approximately exponentially; above optimum it descends sharply.

O'Neill et al. (1972) developed an equation which results in a curve with the necessary form, and at the same time is based on constants which may be readily derived from most experimental data. The equation has the following form:

$$k_T = k_{\max} U^x \exp(xV) \tag{12.28}$$

where

$$U = \frac{T_{\max} - T}{T_{\max} - T_{\text{opt}}} \tag{12.29}$$

and

$$V = \frac{T - T_{\text{opt}}}{T_{\text{max}} - T_{\text{opt}}} \tag{12.30}$$

and

$$x = \frac{W^2 \left(1 + \sqrt{1 + 40/W}\right)^2}{400} \tag{12.31}$$

Here, k_T is the rate of the process at temperature T, k_{max} is the rate at the optimum temperature T_{opt}, and T_{max} is upper lethal temperature. Temperatures are all measured in °C. W is defined as follows:

$$W = (Q_{10} - 1)(T_{\text{max}} - T_{\text{opt}}) \tag{12.32}$$

The Q_{10} value should be estimated from the nearly linear increasing portion of the rate curve. The principal advantage of Equation 12.28 over other exponential equations is that its constants are readily found from plots of most real data. Its disadvantage is the obscure theory behind Equations 12.31 and 12.32. For temperatures above T_{max} it is necessary to set $k_T = 0$, because the equation is not designed to predict values beyond that point.

Logan (1988) reviewed a number of empirical equations that can produce temperature-rate curves resembling those of Figures 12.3 and 12.4. One of the more useful empirical models is partly based on an exponential function like the O'Neill equation above:

$$k_T = k_1 \left(\frac{\tau_1^2}{\tau_1^2 + k_2} - \exp(-\tau_2) \right) \tag{12.33}$$

In this equation, k_T is the rate at temperature T, k_1 and k_2 are empirical constants, and τ_1 and τ_2 are determined from experimental temperature data as

$$\tau_1 = T - T_{\text{min}} \tag{12.34}$$

$$\tau_2 = \frac{T_{\text{max}} - \tau_1}{T_{\text{max}} - T_{\text{opt}}} \tag{12.35}$$

The maximum and optimum temperatures for the reaction rate are defined as in the O'Neill model above. T_{min} is determined from the data, and is the low temperature at which the reaction rate drops effectively to zero. The bracketed part of Equation 12.33 contains two terms which compete to determine the rate. The first term (left-hand) resembles the Michaelis-Menten relationship, and will produce a sigmoid rise in the rate

with increasing temperature. The second, exponential term describes the rate of denaturation of a limiting enzyme, which causes the rate to decline. As temperature increases, the two terms compete, and k_T reaches a maximum value at the optimum temperature. Above this temperature, the second term predominates because its rate of change per degree is much greater than the first term.

The constants k_1 and k_2 may be determined with nonlinear curve-fitting techniques. In actual practice, the values of the constants and the values of the temperature optimum, maximum and minimum may all be evaluated with techniques that permit the least-squares estimation of several coefficients.

Exercise 12-5: Write a program which determines k_T with Equation 12.28 for temperatures between 0 and 48°C . Use the following values for constants in the equation:

$$T_{\text{opt}} = 37 \quad T_{\text{max}} = 42 \quad Q_{10} = 2.5 \quad k_{\text{max}} = 100$$

Output for your program should be a curve showing k_T plotted against temperature in °C.

Exercise 12-6: Moner (1972) obtained the following values for growth rate (inverse of division time) for the ciliated protozoan *Tetrahymena pyriformis* at different temperatures:

°C	Rate	°C	Rate	°C	Rate
14	0.0023	21	0.0073	28	0.0129
15	0.0029	22	0.0087	29	0.0131
16	0.0036	23	0.0093	30	0.0132
17	0.0041	24	0.0100	31	0.0131
18	0.0048	25	0.0110	32	0.0111
19	0.0060	26	0.0117	33	0.0059
20	0.0066	27	0.0121	34	0.0000

Produce a graph of these data with a simple connect-the-dots routine, plotting rate vs. °C. From the plot, estimate the constants needed for the O'Neill model (Equation 12.28).

Write a program as in Exercise 12-5 to draw a curve of k_T vs. temperature from 10°C to 40°C, using your estimates of the constants. On the same graph, plot the actual data points to examine the accuracy of the model equation. You will discover that the

model is quite sensitive to small differences in the estimate of Q_{10}. You should try using various Q_{10} values to improve the fit of the plotted line to the data.

Exercise 12-7: As in Exercise 12-6, produce a rate vs. temperature graph of Moner's (1972) data. From the plot, estimate the values of T_{opt}, T_{max} and T_{min} needed for Logan's Equation 12.33. Then use the CURNLFIT program (Chapter 3) to estimate the constants k_1 and k_2. (To do this, you will need to read in the temperature as x-values and the rates as y-values. Put Equation 12.33 into CURNLFIT using k_T as Y, T as X, and your estimates of T_{min}, T_{max}, and T_{opt} as constants; use k_1 as coefficient A and k_2 as coefficient B.) For initial approximate values needed by CURNLFIT, use 3 times the measured maximum rate for k_1 (coefficient A), and 2 times (T_{max} - T_{min}) for k_2 (coefficient B).

12.6 Modeling Development in Variable Temperatures

Most plants, animals and microbes grow and develop in environments with fluctuating temperatures. Several methods are available for applying rate equations to development in varying temperatures. These models can have important practical application; for example, models for simulating the development of insect eggs or larval stages can permit agricultural controls to be applied most efficiently for maximum effectiveness. We will examine here a simple rate-summation model for predicting development in changing temperatures (Messenger and Flitters 1959, Grainger 1959, Tanigoshi and Browne 1978).

The rate-summation technique estimates duration of development based on the amount of time spent at a given temperature. This time is multiplied by the development rate, determined from constant temperature experiments. The time-rate product indicates how much development occurs during the period. Time-rate products are summed consecutively until the sum reaches unity, at which point the simulated development is complete. Consider a hypothetical example for eggs of a species of insect which experimentally have shown the following development rates at two temperatures:

Constant Temperature	Duration	Rate (1/duration)
10°C	100 hrs	0.01 hr^{-1}
20°C	33.3 hrs	0.03 hr^{-1}

Suppose that an egg is laid in an environment with temperatures alternating between 10°C and 20°C on a 12-hour cycle. If the egg begins to develop at the start of a 12-hour period of 10°C, development will proceed as follows:

Time period	Rate	Development	Sum	Total hrs
12 hrs at 10°C	0.01	0.12	0.12	12
12 hrs at 20°C	0.03	0.36	0.48	24
12 hrs at 10°C	0.01	0.12	0.60	36
12 hrs at 20°C	0.03	0.36	0.96	48
4 hrs at 10°C	0.01	0.04	1.00	52

Exercise 12-8: Write and implement a program based on the rate-summation method to find duration of development when temperature varies. Include in your program a sequence of DATA statements giving length of the period, temperature, and the rate at that temperature. Your program should read a DATA statement, and then calculate the proportion of development that occurs during the period, sum up the development to that time, and check to find if it exceeds 1.00. If not, data for the next period should be read. The portion of the final period required to complete development should be calculated. Output from your program should be in a tabular form, as given above. Test your program using a cycle of alternating 6-hour periods of rates of 0.022 and 0.034 at 12°C and 18°C respectively. Assume egg development begins at the start of a period with the higher rate.

12.7 Model of a Stratifying Lake

The heat-balance model of a lake in Section 12.2 was not very realistic because heat was assumed to be uniform throughout the water column. In fact, most heat is absorbed near the surface and carried down through the water column. One method for modeling lake temperature is to divide the lake vertically into separate compartments. For this method, heat transport is assumed to occur only in the vertical dimension between compartments. Each compartment represents one meter of depth below 1 cm^2 of surface, so the volume of each compartment is 100 cm^3. Heat content of each compartment is measured in calories; in this model, water at 0°C has a caloric content of 0. Thus, temperature of any compartment is its heat content divided by 100 cal $°C^{-1}$.

Solar radiation provides the principal heat input. Absorbed energy contributes to the heat content of a compartment at depth z as described

by a modification of Equation 11.8:

$$(I_a)_z = I_z - I_{z+1} = I_o\left(e^{-\eta(z-1)} - e^{-\eta z}\right) \tag{12.36}$$

where I_a is energy absorbed per unit time, I_z is amount of solar energy reaching the top of compartment z, I_{z+1} is the amount at the bottom, η is the absorption coefficient and I_o is the surface intensity.

Other types of heat transfer between the lake and the atmosphere are assumed to occur only at the surface. The remaining terms in the heat balance model (Equation 12.8) are

$$Q_0 = S - O - E \tag{12.37}$$

where Q_o is the heat transport across the surface per unit of time, S is a sensible heat exchange (convective or conductive), O is heat radiated to the atmosphere, and E is heat transfer by evaporation or condensation.

In addition to the solar energy absorbed, each compartment will have its energy content altered by the transport of heat to the compartment from the adjacent warmer layer, and by the transport of heat from the compartment to the adjacent cooler layer. We will assume that the warmer layer is at a shallower depth, and the cooler layer is deeper. Amount of heat Q_z transported from compartment z to compartment $z+1$ is assumed to be a function of the temperature difference and the eddy diffusivity coefficient, A_z, as follows:

$$Q_z = FA_z\left(T_z - T_{z+1}\right) \tag{12.38}$$

where F is a proportionality constant. In finding heat transfer for the bottom compartment, assume the sediments have the same temperature as the bottom layer of water. The eddy diffusivity coefficient is a function of both the force that produces mixing, i.e. wind, and the force that resists the mixing, i.e. the density gradient; water of greater density lies beneath water of lesser density. The eddy diffusivity coefficient may be approximated with

$$A_z = A_{\min} + 0.9A_{z-1}\exp\left[-G\left(\rho_{z+1} - \rho_z\right)\right] \tag{12.39}$$

A_o will be the wind-induced surface value for eddy diffusivity. (To find A_z for the bottom compartment of water, assume the sediments to have a density value of 1.5). The constant 0.9 describes the exponential decrease in the surface value of eddy diffusivity with increasing depth. G is a constant of proportionality. $A_{\min}$ is the minimum eddy diffusivity, with a value of approximately 0.01 cal cm^{-2}. ρ_z and ρ_{z+1} are the densities of water in compartments z and $z+1$. Water density is a function of temperature, and may be obtained from the following empirical quadratic equation which applies very well over the range of normal lake temperatures:

$$\rho_z = 0.999884 + \left(5.75 \times 10^{-5}\right)T_z - \left(7.27 \times 10^{-6}\right)T_z^2 \tag{12.40}$$

Exercise 12-9: Write a program to simulate the warming of a lake in the spring, assuming an initial temperature of 4°C for all depths. Let the lake have a depth of 20 meters (i.e. 20 compartments), with compartment 1 representing the depth interval 0-1 m. The compartmental temperature values should be stored in a subscripted array. Losses and additions of heat in each compartment may be calculated with the equations above. The calculation of temperatures should be a two-part process. In the first part, the densities for all the compartments are calculated, and then the change in heat content and temperature is calculated for each of the compartments in turn, top to bottom:

$$\Delta T_z = \left[(I_a)_z + Q_{z-1} - Q_z\right]/100 \tag{12.41}$$

with the values for I_a and Q coming from Equations 12.36 and 12.38. For compartment 1, the heat transfer across the surface can be considered to be Q_o (Equation 12.37).

In the second stage the changes are applied to each compartment to update its temperatures:

$$T_z \longleftarrow T_z + \Delta T_z$$

Remember to set the temperature of the sediments (compartment 21) to equal the temperature of compartment 20. Use the following values in setting up your simulation; some represent daily versions of weekly values in Exercise 12 2:

$$I_0 = 350 \quad A_0 = 0.5 \quad O = -20 \quad E = 70$$
$$S = 30 \quad \eta = 0.40 \quad F = 100 \quad G = 2000$$

Run your simulation for 30 days; the surface temperature should approach 26°C. Plot depth-temperature curves at least for times 0 and 30. Your output should consist of a graph showing temperature on the x-axis, and depth on the y-axis. Your graph may be clearer if you plot temperatures of each compartment as connected line segments, rather than as connected points. Graphs for comparison with actual lakes may be found in any textbook of limnology, for example Hutchinson (1957) or Wetzel (1983).

Conclusion

This chapter has introduced you to some representative models of temporal and spatial variation of temperature, and the effect of temperature on biological activity. Although they are interesting in themselves, you will find temperature models like these used in simulations of complex systems. For example, a model of lake temperature could be used in conjunction with a temperature-activity model and a model of photosynthesis as input for a model of algal productivity. Temperature-activity models are essential for simulations in which physiological rates of plants or poikilothermic animals are important components.

CHAPTER 13

COMPARTMENTAL MODELS OF BIOGEOCHEMICAL CYCLING

In several previous chapters we considered various ecological models of growing and interacting populations. In this chapter we will study some ecological models for simulating flow of energy and material through organisms and their environment. These biogeochemical models focus on transfer through components of ecosystems, without considering individual organisms. Our approach will be to examine comparatively simple models that illustrate the principles of biogeochemical models. The techniques of compartmental modeling learned here will be useful in the next several chapters.

13.1 The Concepts of Material and Energy Flow

The concept of flow of materials between different components of the biosphere was worked out early in the twentieth century. For example, Lotka's (1925) box-and-arrow diagram for a global cycle of carbon would be at home (with slightly modified data) in current ecology textbooks. This analytical approach was evidently on Elton's mind as he worked out the first food web for an ecosystem in 1923 (Hutchinson 1978). The same approach influenced Lindeman (1942) in the first attempt to measure energy flow through an ecosystem.

One of the early attempts to obtain a complete, detailed description of energy content and flows in a single ecosystem was Odum's (1957) work on Silver Springs, Florida. The results of this research may be summarized in an energy-flow diagram (Figure 13.1). Similar diagrams are the basis of most ecosystem models.

The diagrams show the amount and direction of flow among components of an ecological community, and between the community and its environment. To develop a complete diagram, one must know for each component the standing crop, and the energy or material inputs and outputs. The organisms in the system may be grouped in a variety of ways; a common division is by trophic level. Depending on the interests and

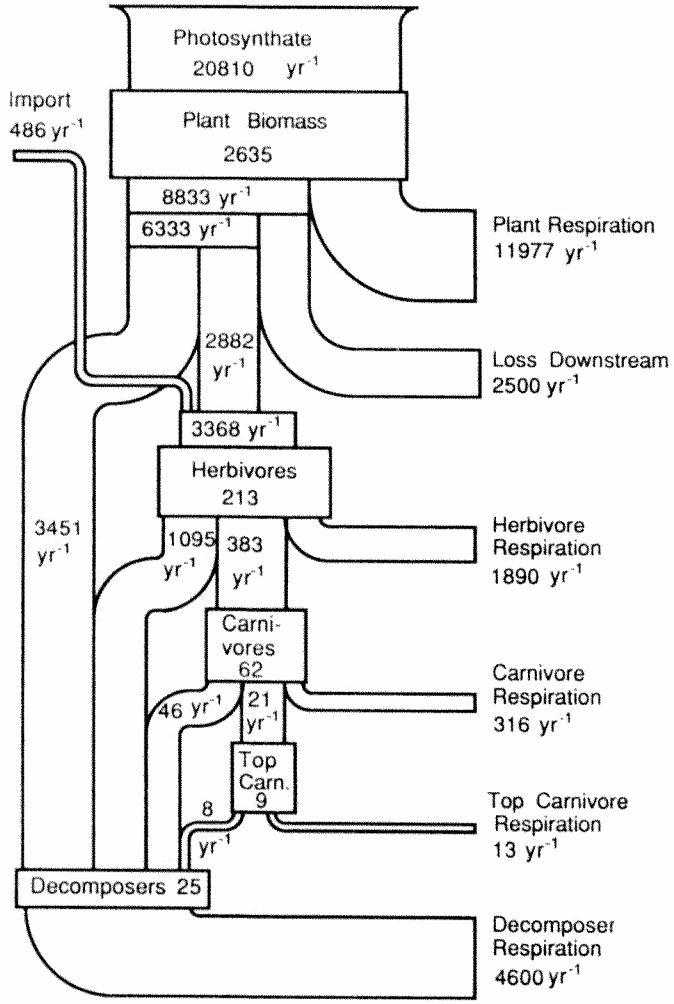

Figure 13.1. An energy diagram of the biological community in Silver Springs, Florida. Based on diagrams by Odum (1957) and by Patten (1971).

objectives of the modeler, a given trophic level may be subdivided in a variety of ways.

13.2 Block Diagrams and Compartment Models

Block diagrams are useful conceptual tools for developing simulations of flow, with each component of the system represented by a rectangular block. The blocks are connected by arrows showing flow of energy or material between components, or between components and the environment. The system may include all biological components of a community, or only a portion, depending upon the modeler's definition of the system. Once the system has been defined, everything else is "environment". Inputs to the system are termed driving or forcing functions. Figure 13.2 is an example of a block diagram.

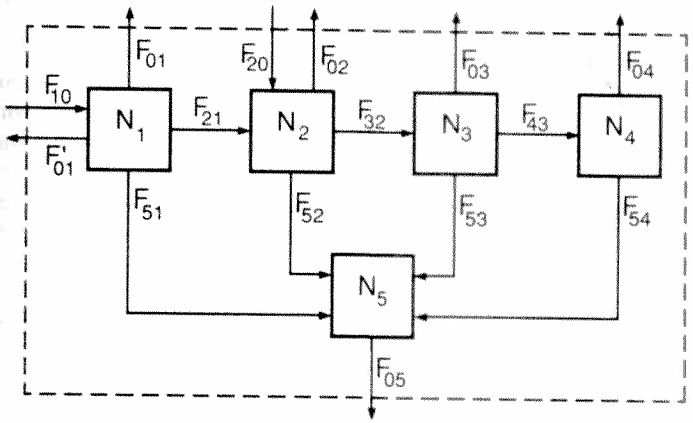

Figure 13.2. A simple block diagram of the Silver Springs energy flow compartmental model, modified from Patten (1971).

The blocks within a diagram may be defined with words. However, letters with subscripts to designate compartments, N_1 and N_2 for example, are more convenient because they may be used directly in writing computer programs. Between compartments, the flows F_{12}, F_{32}, etc., will have subscripts indicating receiving and donating blocks. Conventionally, a subscript of 0 indicates the environment. In this book, the first number in the subscript of a flow will represent the receiving compartment, and the second the source compartment. You should be aware that this subscript order may be reversed by different modelers working in different biological fields. No standardization exists.

In the Silver Springs model (Figure 13.2), N_1 = producers, N_2 = herbivores, N_3 = carnivores, N_4 = top carnivores, and N_5 = decomposers. F_{10} and F_{20} are the two driving flows from the environment. F_{01}, F_{02}, F_{03},

F_{04} and F_{05} represent respiratory losses to the environment from the system. F'_{01} represents the physical loss of plant biomass carried downstream and out of the system by water currents.

Under steady-state conditions, the sum of system inputs, F_{10} and F_{20}, must equal the sum of the system outputs, F_{01}, F_{02}, F_{03}, F_{04}, F_{05} and F'_{01}. Also at steady state, the sum of the inputs to any block must equal the sum of outputs from that block.

The units for the blocks will depend on the system. Usually they express mass or energy on the basis of volume or area. Typical units might be grams of dry weight per square meter, grams of organic carbon per cubic meter, or kilocalories per square meter. The flows will use the same units together with units of time, such as grams per square meter per day, or grams of organic carbon per square meter per year.

A compartmental model is a more formal statement of the block diagram, and includes the equations describing the flows between compartments. Sheppard (1948) apparently was the first to use "compartment" in this sense (Godfrey 1983). The flows or fluxes are used in the equations to provide an energy or material balance for each compartment. The rate of change for each compartment is found by adding the flows into the compartment and the flows out of the compartment. For the Silver Springs model these are

$$\frac{dN_1}{dt} = F_{10} - F_{21} - F_{01} - F_{51} - F'_{01} \tag{13.1}$$

$$\frac{dN_2}{dt} = F_{21} + F_{20} - F_{02} - F_{32} - F_{52} \tag{13.2}$$

$$\frac{dN_3}{dt} = F_{32} - F_{43} - F_{03} - F_{53} \tag{13.3}$$

$$\frac{dN_4}{dt} = F_{43} - F_{04} - F_{54} \tag{13.4}$$

$$\frac{dN_5}{dt} = F_{51} + F_{52} + F_{53} + F_{54} - F_{05} \tag{13.5}$$

Each flow is defined by an equation which usually involves a rate coefficient. We will designate the rate coefficients as f_{ij}. A large number of equations could be used to model flow between compartments, but only a few useful equations are encountered frequently. Some of these are described in Table 13.1. A variety of other examples may be found in Godfrey (1983).

$F_{ij} = k$	Flow from compartment j to i is constant, and is independent of time and system state.
$F_{ij} = f_{ij}N_j$	Flow to i is proportional to the content of j. This is a linear equation with control by the donor compartment only, with rate constant f_{ij}.
$F_{ij} = f_{ij}N_i$	Flow to i is proportional to the content of i. This is a linear equation describing control of flow by the receptor compartment.
$F_{ij} = f_{ij}N_iN_j$	Flow to i is controlled by both donor and receptor compartments in a cross-product manner. This is the mass-action approach. The equation is nonlinear.
$F_{ij} = f_{ij} \cdot f(\text{time})$	Flow from j to i is a function of time. An example is a sine function (Equation 11.2).
$F_{ij} = f_{ij}N_i(1 - g_{ij}N_i)$	Flow from j to i is controlled by a positive linear term and a negative non-linear term, much like the logistic equation.
$F_{ij} = \dfrac{f_{ij}N_i}{K + N_i}$	Flow from j to i is limited with a hyperbolic term as in Michaelis-Menten kinetics.

Table 13.1. Some useful equations for describing flow between compartments. F_{ij} is the instantaneous flow to compartment i from compartment j, and f_{ij} is the rate coefficient. N_i indicates the content of compartment i.

Compartment models of the type described here are often implemented on computers by solving the system of equations with matrix algebra. This method will be discussed in Chapter 16. For the present, we will solve the equations with a direct approach. Because most of the equations of flow are functions of the size of the compartments, it is necessary

to use the two-stage numerical approach with Euler integration. For clarity of programming, the first stage should be separated into two parts as described in Section 6.2. That is, the various flows F will all be calculated, and then the net changes of content for each compartment will be determined to complete the first stage. Then, following the usual second stage procedures, values of the compartments will be updated.

13.3 The Silver Springs Model

We will continue working with the Silver Springs model as an example. It is not better than similar and more recent models. However, it is familiar and relatively uncomplicated, and it still appears in general ecology textbooks. The set of equations given in this section define the flows in the block diagram of Figure 13.2, and have been modified from Odum (1957) and Patten (1971):

(A. Forcing:)
$$F_{10} = M + R\sin\left(2\pi\frac{(T-11)}{52}\right)$$

$$F_{20} = k$$

F_{10} is the energy input from photosynthesis, assumed to be proportional to light intensity. M is the annual mean photosynthesis, and R is the range of the annual fluctuation around the mean. F_{20} is the energy in 70 loaves of bread fed daily to catfish by the tourist concession at the springs.

(B. Feeding:)
$$F_{21} = \tau_{21}N_1$$

$$F_{32} = \tau_{32}N_2$$

$$F_{43} = \tau_{43}N_3$$

Feeding is donor-dependent in this system, with τ_{ij} the linear coefficient having units of inverse weeks (wk^{-1}).

(C. Mortality:)
$$F_{51} = \mu_{51}N_1$$

$$F_{52} = \mu_{52}N_2$$

$$F_{53} = \mu_{53}N_3$$

$$F_{54} = \mu_{54}N_4$$

Here μ_{ij} is a coefficient of donor-dependent mortality, with units of wk^{-1}.

(D. Respiration:)
$$F_{01} = \rho_{01}N_1$$

$$F_{02} = \rho_{02}N_2$$

$$F_{03} = \rho_{03}N_3$$

$$F_{04} = \rho_{04}N_4$$

$$F_{05} = \rho_{05}N_5$$

Here ρ_{ij} is a coefficient of donor-dependent respiration, with units of wk^{-1}.

(E. Export:)
$$F'_{01} = \lambda_{01}N_1$$

λ_{01} is a coefficient of the loss downstream of small plants and pieces of plants that break loose from the plants that grow in the Silver Spring system. The coefficient has units of wk^{-1}.

After the F_{ij} values are calculated with the equations given above, the first stage in the two-stage Euler procedure is completed with the calculation of the ΔN_i values:

$$\Delta N_1 = (F_{10} - F_{21} - F_{51} - F_{01} - F'_{01})\,\Delta t$$

$$\Delta N_2 = (F_{20} + F_{21} - F_{32} - F_{52} - F_{02})\,\Delta t$$

$$\Delta N_3 = (F_{32} - F_{43} - F_{53} - F_{03})\,\Delta t$$

$$\Delta N_4 = (F_{43} - F_{54} - F_{04})\,\Delta t$$

$$\Delta N_5 = (F_{51} + F_{52} + F_{53} + F_{54} - F_{05})\,\Delta t$$

The second stage of the Euler integration is completed as usual, with

$$N_i \longleftarrow N_i + \Delta N_i$$

Exercise 13-1: Write and implement a program to simulate energy flow through Silver Springs using the model equations above. For

the various compartment sizes and flows, use values given below derived from Odum (1957). The values of mean annual standing crop given in Figure 13.1 (units of kcal m^{-2}) are suitable for initial compartment sizes:

$$N_1 = 2635 \qquad N_2 = 213 \qquad N_3 = 62 \qquad N_4 = 9 \qquad N_5 = 25$$

The values of rate coefficients (units of yr^{-1}) can be calculated by inserting yearly values for the flows and for standing crops into the flow equations for mortality, feeding, respiration and export. This process yields coefficients as follows:

$$\mu_{51} = 1.310 \qquad \mu_{52} = 5.141 \qquad \mu_{53} = 0.742 \qquad \mu_{54} = 0.889$$
$$\tau_{21} = 1.094 \qquad \tau_{32} = 1.798 \qquad \tau_{43} = 0.339$$
$$\rho_{01} = 4.545 \qquad \rho_{02} = 8.873 \qquad \rho_{03} = 5.097 \qquad \rho_{04} = 1.444$$
$$\rho_{05} = 184.0 \qquad \lambda_{01} = 0.94$$

For the driving functions, use the following values:

$$k = 486 \text{ kcal m}^{-2} \text{ yr}^{-1} \qquad R = 175 \text{ kcal m}^{-2} \text{ wk}^{-1}$$
$$M = 400 \text{ kcal m}^{-2} \text{ wk}^{-1}$$

Most of the rate coefficients above are based on annual flows through the system; weekly values may be found with division by 52. Use weeks as the time unit for your simulation, with $\Delta t = 0.1$ week as the unit for Euler integration. Larger Δt values will produce unstable results.

Write your program to plot the contents of each compartment for each week, including initial values. Your output will be a graph with five separate lines, each showing the content of a model compartment.

After you have entered the program into your computer, make an initial trial run, setting $R = 0$. This procedure will keep F_{10} constant. The system should tend rapidly to a steady-state condition. If it does not, then check your program for errors.

After this initial check, carry out a 3-year simulation, beginning with the first week in January. Set $R = 175$ kcal m^{-2} wk^{-1}.

Exercise 13-2: A crude simulation of ecological succession may be obtained with the model above by setting the solar input to a constant value ($R = 0$) and reducing the starting size of all compartments to some minimum value (such as 5 kcal m^{-2}). Allow the simulation

of the system to proceed for about 150 weeks to stabilize. Again use $\Delta t = 0.1$ week.

Exercise 13-3: Modify the Silver Springs model above by employing nonlinear feeding equations as follows:

$$F_{21} = \tau'_{21} N_1 N_2$$

$$F_{32} = \tau'_{32} N_2 N_3$$

$$F_{43} = \tau'_{43} N_3 N_4$$

Numerical values for the coefficients may be found by inserting the values for flows and standing crop sizes (Figure 13.1) and solving. This produces the following values for the coefficients:

$$\tau'_{21} = 0.00513 \qquad \tau'_{32} = 0.0290 \qquad \tau'_{43} = 0.0376$$

As in Exercise 13-1, run the simulation for a 3-year period, plotting the energy content of the five compartments. The larger excursions of the compartment contents produced by the nonlinear flows should be apparent.

13.4 Global Carbon-Cycle Model

The increased concentration of carbon dioxide that has been measured in the earth's atmosphere has caused concerns about global warming. There exist real controversies on the relative roles of burning fossil fuels and clearing tropical forests in producing the increase. The relative ability of terrestrial plants and the oceans to serve as reservoirs for the increase in carbon is also controversial. Complex compartmental models are important tools in working with analysis and prediction of the carbon cycle. Bolin (1981) has outlined a simple model of the carbon cycle that shows many of the expected characteristics of the cycle. We will use a modified version of this model as an introduction to the important subject of carbon cycle modeling, and as a further illustration of ecological compartment models.

In this model, carbon is distributed among seven compartments (Figure 13.3). The principal pool of the atmosphere can exchange carbon with both oceanic and terrestrial components. The oceans are represented by only two compartments, one for the mixed layers near the surface that come into contact with the atmosphere, and another for the deeper, more

isolated waters. The terrestrial component is made up of four compartments: short-lived vegetation with a rapid carbon turnover, including annual plants and vegetative parts such as leaves; long-lived vegetation, particularly the woody trunks, stems and roots of trees; detritus, defined as dead and decomposing organic matter, sometimes called litter, duff, or humus; and organic material in the soil.

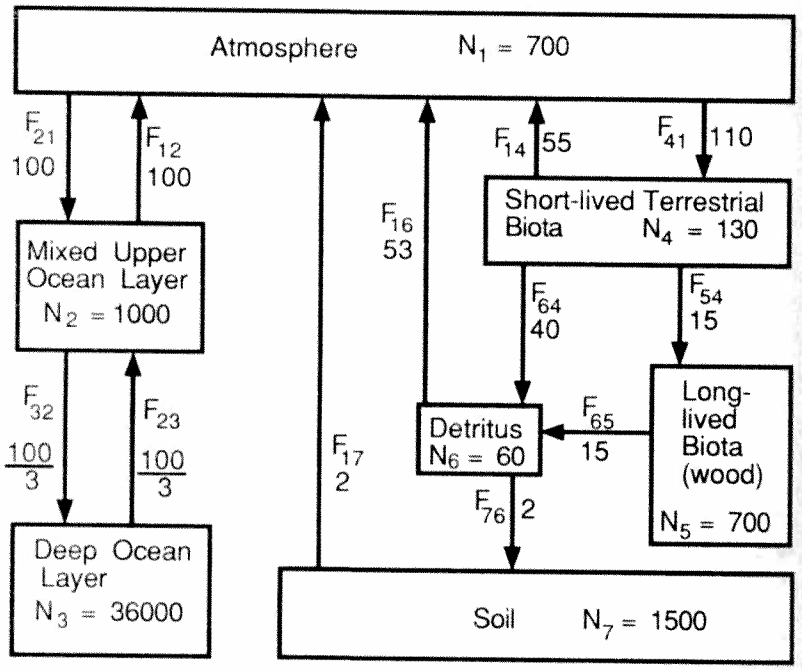

Figure 13.3. Block diagram of the equilibrium carbon cycle, modified from Bolin (1981). Pool sizes are in units of 10^{15} grams (=gigatons; GT). Transfers between compartments are in units of GT year^{-1}.

With two exceptions, the flows between compartments are linear, first-order, donor-controlled flows. That is, flow to compartment i from compartment j is described with

$$F_{ij} = k_{ij} N_j \tag{13.6}$$

The two exceptions are the flows representing uptake of atmospheric carbon by terrestrial plants, and the transfer of carbon dioxide from the ocean

to the atmosphere. In the first case, flow between plants and the atmosphere is controlled by both donor and receptor compartments. Within broad limits, a larger biomass of plants should be able to take up more atmospheric carbon than a smaller quantity of plants. Also, an increase in atmospheric CO_2 may stimulate plant growth, so that the transfer to plants may occur at a greater rate. However, the transfer is not directly proportional to the concentration of atmospheric CO_2; that is, a doubling of the CO_2 concentration would almost certainly not double the flow of carbon. Bolin (1981) suggested a linearized version of a nonlinear equation. Yearsley and Lettenmaier (1987) used the following nonlinear equation for this transfer:

$$F_{41} = k_{41} N_4 \left(1 + \beta \ln \frac{N_1}{(N_1)_0}\right) \tag{13.7}$$

Here, $(N_1)_0$ is the equilibrium value for the atmospheric carbon, N_1 is the current concentration, and β is a photosynthetic coefficient. The equation is semi-empirical, and indicates that uptake of atmospheric carbon is proportional to the amount of plant material when the atmosphere is at the equilibrium level of 700 GT. As atmospheric carbon rises above the equilibrium level, plants will be able to take up only a part of the increased atmospheric CO_2 .

The second instance of nonlinear flow is the transfer from the ocean to the atmosphere. This transfer is made complex by the chemical buffering system of the ocean. Bolin (1981) suggested that the flow could be described with

$$F_{12} = k_{21} \left((N_1)_0 + \xi \frac{(N_1)_0}{(N_2)_0} [N_2 - (N_2)_0]\right) \tag{13.8}$$

The equilibrium values for the atmosphere and mixed-layer are given with $(N_1)_0$ and $(N_2)_0$. The current value of the mixed layer is N_2, and ξ is a buffering constant. k_{21} (not a misprint) is the constant for the flow to compartment 2 from 1. This equation may be written in a much simpler form when appropriate constants are inserted. The result is:

$$F_{12} = N_2 - 900 \tag{13.9}$$

This form of the equation will hold for all reasonable values of an increase in the CO_2 content of the mixed layer. Elaborations of Bolin's basic model and more complex models may be found in papers by Yearsley and Lettenmaier (1987), Mulholland et al. (1987), and Detwiler and Hall (1988).

Exercise 13-4: On your computer, implement the global carbon model from the above information. As an early step in your program, solve for the transfer coefficients for the various flows (except F_{12} and F_{41}) using Equation 13.6. That is, find $k_{ij} = F_{ij}/N_j$. Use the whole-number equilibrium values in Figure 13.3. Because the model is sensitive to errors in the fourth or fifth significant digit for these constants, it is easiest to have the computer solve for these k_{ij} values and retain them.

Write your program using two-stage Euler integration, following the procedure described in Sections 13.2 and 13.3. That is, first calculate all the flows F_{ij} using Equation 13.6, but for F_{12} use Equation 13.9, and for F_{41} use Equation 13.7 with $\beta = 0.10$ and $k_{41} = 110/130$. Then find all the compartmental changes ΔN_i, and finally perform the updates for the new values of N_i. For this simulation set $\Delta t = 0.1$ year.

Begin your simulation with the equilibrium pool values from Figure 13.3. Plot the values of the various pools N_i through time for 20 years to be sure they remain at equilibrium.

After you are sure your program is working with the equilibrium values, alter your program so that a slug of 10 GT of carbon is added to the atmosphere at the beginning of year 10. This simulates the burning of a large amount of fossil fuel in that year. Follow the result of the perturbation for 90 years. For this simulation, the graphical output should show the departure of each pool from its equilibrium value, rather than pool size. That is, your x-axis should run from 0 to 100 years, and your y-axis from -10 to +10 GT.

Exercise 13-5: Modify the program of Exercise 13-4 to simulate a single incident of massive destruction of forest and release of carbon by burning of the wood. This is easily done by removing 10 GT from the compartment of long-lived biota at the same time that 10 GT is added to the atmosphere.

Exercise 13-6: For more than a century atmospheric carbon has been increasing principally because of combustion of fossil fuels including coal and oil. The amount of carbon added to the atmosphere each year has also increased. The amount of carbon from fossil sources added to the atmosphere each year by human activity may be described quite accurately with

$$\text{GT added each year} = 0.5\ e^{0.03t}$$

where t is the number of years since 1900 (Rotty 1981).

Modify your program from Exercise 13-4 to simulate the addition of carbon from fossil fuel combustion for an 80 year period, 1900-1980. At least initially most of the added carbon accumulates in the atmospheric pool N_1. As output from your program, plot the cumulative carbon input to the atmosphere from fossil fuel combustion, and the change in the atmosphere from equilibrium. Then alter your program so that it will plot the distribution of the added carbon among the seven pools over the 80-year period. Initially, almost 100% of the added carbon will be in the atmosphere; this should decline to about 30% after 80 years, with 70% distributed among the other compartments.

13.5 Simulated Food Chain

Elliot et al. (1983) based a model of a planktonic grazing food chain on a general model of predation developed by Wiegert (1975, 1979). The model is instructive because it attempts to include a number of realistic factors in the transfer of material through the food chain. Some of these factors you have encountered previously in Chapters 7 and 8 for homogeneous populations, including self-limitation of population size, saturation of predators, and minimal prey density. The basic four-compartment model of the planktonic food chain is shown in Figure 13.4.

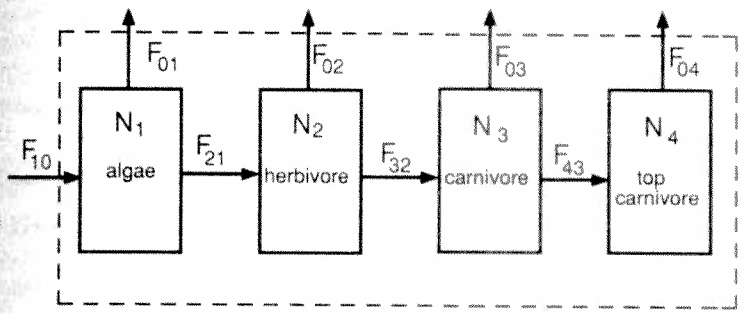

Figure 13.4. A block diagram for a simple 4-compartment model of a planktonic grazing food chain.

The model is simplified so that non-grazing losses from each compartment are combined in a single term. That is, rates of respiration, non-grazing mortality, etc., are all lumped together in a single factor to model loss to the environment. This flow to the environment from each of the four compartments is given by

$$F_{0i} = \lambda_{0i} N_i \qquad (13.10)$$

where N_i is compartmental density (measured in units of mass) and λ_{0i} is the rate constant for loss, with units of time^{-1}.

The system is driven by a flow into compartment 1 from the environment, F_{10}. This flow will be a constant in the simulation described here. However, it may be made a function of time, for example a sine function as in the Silver Springs simulation above.

The predatory or grazing transfers of mass between all the compartments are modeled with equations having the same form. The equations include terms for both donor and receptor control:

$$F_{21} = \tau_{21} N_2 \left[D_{21} R_{21} \right]_+ \tag{13.11}$$

$$F_{32} = \tau_{32} N_3 \left[D_{32} R_{32} \right]_+ \tag{13.12}$$

$$F_{43} = \tau_{43} N_4 \left[D_{43} R_{43} \right]_+ \tag{13.13}$$

In these equations τ_{ij} is the feeding rate constant for grazing transfer to compartment i from j. It may also be thought of as the rate constant for exponential growth of N_i, whenever D_{ij} and R_{ij} are held constant.

The + subscript for the bracketed term is used to indicate that this term must be positive or zero. That is,

$$[x]_+ = x \quad \text{if} \quad x \geq 0$$

$$[x]_+ = 0 \quad \text{if} \quad x < 0$$

(Note that this is not equivalent to absolute value.) In these equations, this convention prevents the flow from being negative, and having the prey feeding on the predator. (The terminology is easily programmed in BASIC with the statement IF X < 0 THEN X = 0.)

The explanations of the D and R components of these equations will be given for the specific example of F_{21}, the flow to compartment 2 from compartment 1. Only the subscripts need to be altered to find the equivalent terms for F_{32} and F_{43}.

D_{21} is a term for the donor control of flow to compartment 2 from 1. The term may take several forms, including $D_{21} = 1$ to indicate simple receptor control of flow. Wiegert (1979) suggests the following as a realistic expression:

$$D_{21} = \left[1 - \left(\frac{\alpha_{21} - N_1}{\alpha_{21} - \gamma_{21}} \right)_+ \right]_+ \tag{13.14}$$

The function of the + subscripts is important and is described above. α_{21} is a constant that represents a saturating density of prey N_1. When prey density N_1 is greater than α_{21}, then D_{21} is equal to 1. Thus, F_{21} in Equation 13.11 will not be decreased because of a lack of prey. γ_{21} is a constant that represents some minimal density of prey. If prey density N_1 drops below γ_{21}, then D_{21} drops to zero. In this case, F_{21} in Equation 13.11 will become zero also, and there will be no feeding on the prey. (γ_{21} may represent for example the number of hiding places for prey, where they can be safe from predation.)

R_{21} is the term in Equation 13.11 for receptor control of the flow F_{21}. In this model it describes self-limitation of the predator population, with a modified logistic function. Weigert's (1979) expression was:

$$R_{21} = \left[1 - \left(1 - \frac{\lambda_{02}}{\tau_{21}} \right) \left(\frac{N_2 - \alpha_{22}}{\gamma_{22} - \alpha_{22}} \right)_+ \right]_+ \tag{13.15}$$

Again, the + subscripts are important. λ_{02} is the rate constant for loss from compartment 2. α_{22} is a constant indicating the density at which predators begin to interact and to compete with each other. When N_2 exceeds α_{22}, R_{21} drops below 1 because of the predators' self-interference. γ_{22} represents the limiting maximum density of predators, so that R_{21} will decline as N_2 approaches γ_{22} .

This model system is extremely flexible, and can be used to simulate many features of the grazing food chain of aquatic ecosystems. The equations and constants may be modified to provide a variety of possible simulations, involving changes in refuge size, maximal densities, predation rates, and loss rates. These variations will produce widely varying results. The density of compartments may reach equilibrium, or oscillate in stable and unstable ways.

Exercise 13-71: Write a program for simulating planktonic grazing with the 4-compartment model of food chains described above. As described in Section 13.2, use a two-stage Euler integration, with the first stage subdivided into two parts. That is, for stage one first calculate the flow rates between components of the system with Equations 13.10 through 13.15, and then find the ΔN_i values by summing rates. For stage two, update the compartment values. It should be adequate to set $\Delta t = 0.1$ for the simulation of planktonic grazing.

The following coefficients were suggested by Elliot et al. (1983) as reasonable estimates for the grazing planktonic food chain in some freshwater systems:

$\lambda_{01} = 0.10$ $\lambda_{02} = 0.46$ $\lambda_{03} = 0.37$ $\lambda_{04} = 0.20$
$\tau_{21} = 1.15$ $\tau_{32} = 0.74$ $\tau_{43} = 0.27$
$\alpha_{21} = 20.0$ $\alpha_{32} = 15.0$ $\alpha_{43} = 5.0$
$\gamma_{21} = 5.0$ $\gamma_{32} = 2.0$ $\gamma_{43} = 0.50$
$\alpha_{22} = 10.0$ $\alpha_{33} = 5.0$ $\alpha_{44} = 1.0$
$\gamma_{22} = 30.0$ $\gamma_{33} = 20.0$ $\gamma_{44} = 20.0$

Use a constant input for this system of $F_{10} = 20.0$. For initial values of the compartments, use the following:

$N_1 = 10.0$ $N_2 = 2.0$ $N_3 = 5.0$ $N_4 = 1.0$

In this simulation, units of time and units of mass are arbitrary. As output for this simulation, plot values of the compartmental densities N_i against time for 0 to 240 units of time.

Exercise 13-8: Modify the simulation of Exercise 13-7 to show the effect of limiting the maximum density of the top carnivore. This modification might be needed for a simulation with a species that is more territorial, for example. Thus, in your program reduce the constant for maximum top carnivore density, γ_{44}, from 20 to 10 units and then rerun the simulation.

Conclusion

This chapter has introduced you to some of the concepts and techniques of working with models of material and energy flow through large-scale systems. In succeeding chapters you will work with compartmental models of smaller systems, and many of the methods you have learned here will be useful. The direct two-stage Euler approach has been described for implementing these models on the computer. The more elegant matrix approach will be taken up in Chapter 16. The three examples described in this chapter were relatively simple and designed to promote understanding of methodology. However, the same techniques may be applied to more complex, diverse systems. The simulation programs become longer, and the results less intuitively obvious, but the fundamental methods still apply.

CHAPTER 14
DIFFUSION MODELS

In the compartmental ecological systems of the previous chapter, the mechanisms of transport of material and energy between compartments were relatively straightforward. In physiological models, the mechanisms of transport are frequently the subject of interest. These mechanisms usually fall into three general categories: diffusion, active transport, and fluid flow. Each of these presents different problems requiring different modeling approaches. We will consider the first two mechanisms in this chapter. Fluid flow and other transfers among physiological compartments will be discussed in the next chapter.

A solution is made by dissolving some matter (solute) in a fluid (solvent). A solution may be described by its mass concentration, which is the mass of the solute per unit volume of solution. Molecules of solute are dispersed through the solvent by diffusion, a result of the thermal movements of the solvent molecules colliding with the molecules of solute.

14.1 Transport by Simple Diffusion

A simple model of transport of material by diffusion between a single compartment and an unchanging environment was discussed in Section 1.5. Frequently we are interested in diffusion between compartments, for example between two adjacent cells (Figure 14.1). Across a membrane separating the two compartments, net material transfer will proceed from the compartment of higher concentration to the compartment of lower concentration. The rate of transfer will be proportional to the difference in concentrations. For the simple model here, we will assume constant compartmental volumes and uniformity of concentration inside compartments.

The following equation describes forward diffusion from compartment i to j:

$$\left(\frac{dQ_i}{dt}\right)_f = \frac{-kQ_i}{V_i} \tag{14.1}$$

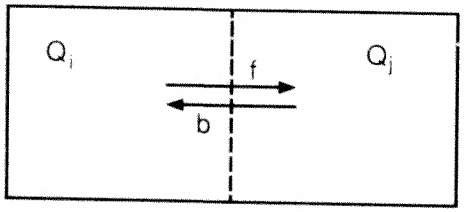

Figure 14.1. Diagram representing simple transport between two cells, with Q representing concentration. The direction of diffusion is indicated with f (forward) and b (back), relative to compartment i.

Q_i is the mass of some diffusing substance in compartment i, V_i is the volume of compartment i, and k is the rate constant for diffusion. Note that concentration is Q_i/V_i, and that k has units of volume (unit time)$^{-1}$. A negative is included to indicate a loss of material from compartment i.

When an amount of material exists in compartment j, there will occur a reverse or back diffusion from j to i. The effect of this on compartment i is described with

$$\left(\frac{dQ_i}{dt}\right)_b = \frac{kQ_j}{V_j} \tag{14.2}$$

The net rate of diffusion of the substance from compartment i is the sum of these two equations:

$$\left(\frac{dQ_i}{dt}\right)_{net} = \left(\frac{dQ_i}{dt}\right)_f + \left(\frac{dQ_i}{dt}\right)_b = k\left(\frac{Q_j}{V_j} - \frac{Q_i}{V_i}\right) \tag{14.3}$$

The change in amount of substance in each compartment may be solved with the usual procedure for two-stage simple Euler numerical integration. The first stage requires two equations:

$$\Delta Q_i = k\left(\frac{Q_j}{V_j} - \frac{Q_i}{V_i}\right)\Delta t \tag{14.4}$$

$$\Delta Q_j = k\left(\frac{Q_i}{V_i} - \frac{Q_j}{V_j}\right)\Delta t \tag{14.5}$$

The second stage involves the usual update procedure:

$$Q_i \leftarrow Q_i + \Delta Q_i \tag{14.6}$$

$$Q_j \leftarrow Q_j + \Delta Q_j \tag{14.7}$$

Exercise 14-1: Write and implement a program to simulate diffusion of a substance between two compartments of a hypothetical system. Initally only one of the compartments will contain a quantity of the diffusing substance. Use the following as constants in your simulation:

$$k = 0.75 \text{ ml min}^{-1} \qquad V_j = 60 \text{ ml} \qquad V_i = 20 \text{ ml}$$

For initial values, set $Q_j = 0$ mg and $Q_i = 100$ mg. Use a Δt value of 0.1 with simple Euler integration. As output, produce a graph which shows the concentration of substance in each compartment, from time 0 to a few minutes past the point at which steady-state occurs.

14.2 Linear Diffusion Gradient

The following simulation is an elaboration of the two-compartment model above. It provides a method for studying the pattern of concentration which results when solutes diffuse across a boundary that is initially quite sharp. Such a boundary might occur, for example, when a lump of sugar is dropped into a cup of tea and allowed to dissolve without stirring.

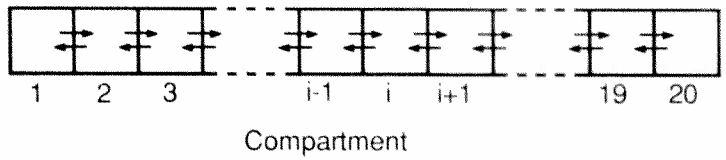

Figure 14.2. Diffusive transport along a linear gradient of 20 compartments.

Assume that the diffusion system is represented by a series of compartments (Figure 14.2). For simplicity in simulation, assume also that the subcompartments are all of the same unit volume, i.e. $V_i = 1$. The net flux from compartment i to adjacent compartment $i+1$ will be described by Equation 14.3, with slightly modified terminology:

$$F_i = k\left(C_i - C_{i+1}\right) \tag{14.8}$$

where F_i is net flux from compartment i to $i+1$, C_i and C_{i+1} are the concentrations (Q/V) in compartments i and $i+1$, and k is the diffusion rate constant as above.

The diffusion along the gradient of compartments can be found with two-stage Euler numerical integration. In stage one, all flows first are found between all compartments with Equation 14.8. Then as the second part of stage one, the net change is calculated for each compartment with

$$\Delta C_i = (F_{i-1} - F_i)\,\Delta t \tag{14.9}$$

For the second stage of the Euler procedure, concentrations in each compartment are found with the usual Euler equation for up-dating:

$$C_i \leftarrow C_i + \Delta C_i \tag{14.10}$$

Exercise 14-2: Write and implement the simulation of diffusion along a linear gradient of 20 compartments. Set $k = 0.1$. Use a Δt value of 0.1. Begin your simulation with $C_i = 100$ for values of i from 1 to 10, and $C_i = 0$ for $i = 11$ to 20. Output should consist of a graph showing compartment number (distance) on one axis and concentration on the other. Show these plots of concentration after 0, 20, 40, 60, 80 and 100 time units. The equations above are set up to permit easy use of subscripted variables. Set $F_0 = 0$ and $F_{20} = 0$.

14.3 Osmotic Pressure Model

Osmosis is a special case of diffusion in which the solvent, usually water, is the primary diffusing substance. The following model of osmotic pressure is based on the classical osmosis experiment, illustrated in Figure 14.3. The movement of water during osmosis is simply diffusion along a concentration gradient from high concentration of water towards a lower concentration of water. Only water can pass through the membrane; the large molecules of the solute are restricted to the osmometer chamber. Rate of water diffusion into the chamber is described by the equation

$$\text{Flow in } = k_i\,(W_e - W_i) \tag{14.11}$$

The diffusion rate constant k_i is a function of the properties of the membrane, including its thickness and area. W_e is the concentration of water outside the compartment expressed as a mole fraction, usually 1.0, which indicates pure water. W_i is the mole fraction of water inside the membrane. If w is the number of moles of water and s is the number of moles of solute per unit volume inside the compartment, then

$$W_i = \frac{w}{(w+s)} \tag{14.12}$$

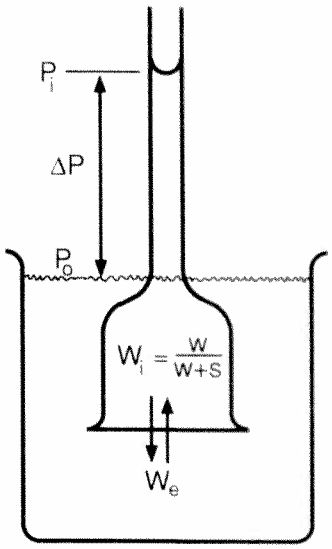

Figure 14.3. Diagram of the apparatus for the classic experiment for determining osmotic pressure. Terminology is defined in the text.

Substituting this into Equation 14.11 gives

$$\text{Flow in } = k_i \left(W_e - \frac{w}{w+s} \right) \tag{14.13}$$

The backflow of water across the membrane is the result of a difference in hydrostatic pressure, and is described by the equation

$$\text{Flow out } = k_h(\Delta P) \tag{14.14}$$

where k_h is a constant relating the flow rate to the difference in hydrostatic pressure across the membrane (ΔP; see Figure 14.3). k_h will vary with the area, thickness, and porosity of the membrane and with the fluid viscosity. Pressure difference ΔP will partly depend on the geometry of the manometer. Equation 14.14 may be simplified by basing the outflow on the amount of water in the chamber relative to the initial amount, which will be adjusted so that $\Delta P = 0$. This will give the following:

$$\text{Flow out } = k_o(w - w_0) \tag{14.15}$$

where w is the amount of water in the chamber at any time t, and w_0 is the initial amount of water when $\Delta P = 0$. k_o is k_h multiplied by a proportionality constant.

Equations 14.13 and 14.15 can be combined to produce an equation for net flow across the membrane as a result of two processes. The equation in words is:

Net flow of water = flow in (by diffusion)
- flow out (due to hydrostatic flow)

With the terms used above the equation is:

$$\frac{dw}{dt} = k_i \left(W_e - \frac{w}{w+s} \right) - K_o(w - w_0) \qquad (14.16)$$

This equation can be solved by the usual two-stage Euler procedure for numerical integration. After the system reaches equilibrium, when net flow is zero (flow in = flow out),

$$k_i \left(W_e - \frac{w}{w+s} \right) = k_o(w - w_0) \qquad (14.17)$$

Exercise 14-3: Write and implement a program to simulate a determination of osmotic pressure using the model above. Use the following constants and initial values:

$$k_i = 20 \qquad k_o = 0.30 \qquad W_e = 1 \qquad w_0 = 55 \qquad s = 1$$

For the Euler integration, let $\Delta t = 0.1$. The backflow from Equation 14.15 may be converted to pressure (atmospheres) with multiplication by a factor of 62.199. This in turn may be converted to inches of water with multiplication by a factor of 414, or to mmHg by a factor of 760.

Run your simulation until the net flow across the membrane is almost zero. At this point, the atmospheric pressure is the osmotic pressure. As output, plot osmotic pressure and net flow from time = 0 to equilibrium.

14.4 Countercurrent Diffusion

Countercurrent diffusion has evolved in a number of species as an efficient mechanism to transport materials or heat from one fluid-carrying vessel to another. One example is the special anatomical relationship

between the loops of Henle in the kidney nephron and the medullary interstitial fluid (Guyton 1971). Another example is the system that whales, seals and birds use to transfer heat between arterial and venous circulation in their feet and flippers. This system, called the *rete mirabile*, is designed for the efficient conservation of heat. Both of these mechanisms have two counter-flowing vessels close together, so that materials or heat may be exchanged through simple diffusion. The countercurrent system maximizes the intensity of the gradient at all points where diffusion is occurring.

An effective model of countercurrent diffusion may be based upon two series of parallel compartments, separated by a membrane which permits transport. The A compartments represent one vessel through which fluid passes and the B compartments represent another vessel parallel to A.

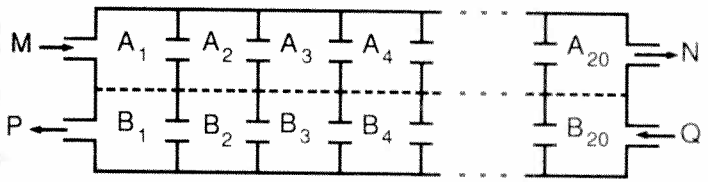

Figure 14.4. Conceptual diagram for a model to simulate countercurrent flow. The terminology is explained in the text.

Figure 14.4 illustrates the model system using terminology that simplifies programming. The diffusion between any pair of compartments A_j and B_j may be described by Fick's Law, which states that the rate of diffusion across a thin membrane is proportional to the area of the membrane, the difference in concentrations, and a constant of permeability:

$$F_{BA} = p\,a\,(A_j - B_j) \qquad (14.18)$$

where F is the flow to compartment B_j from compartment A_j, p is the permeability constant, and a is the membrane area. A_j and B_j designate not only the compartments, but represent the concentrations of the diffusing substance in the compartments. The simplifying assumptions associated with the model are (1) membrane area and permeability constants are the same for all compartments; (2) volume of each compartment is constant and equal to unity, so that concentrations and amounts in each compartment are equivalent.

Movement of fluid in the vessels is assumed to occur by plug flow. This flow is modeled by having the material in each of the A compartments

move one compartment to the right for each time unit. Simultaneously material in each B compartment moves one compartment to the left for countercurrent flow. Simulation of countercurrent flow involves two sets of equations, one set for calculating diffusion flow, and a second set for the plug flow of fluids through the system. Diffusion may be simulated with the usual two-stage Euler procedure. As part of the first stage the diffusion between each pair of compartments is found with Equation 14.18, and then the changes in each compartment are found with

$$\Delta A_j = -F_{BA}\Delta t \tag{14.19}$$

$$\Delta B_j = +F_{BA}\Delta t \tag{14.20}$$

Each compartment is updated as usual with

$$A_j \leftarrow A_j + \Delta A_j \tag{14.21}$$

$$B_j \leftarrow B_j + \Delta B_j \tag{14.22}$$

The procedure for programming plug flow involves the use of the following sequence for the A compartments:

$$N \leftarrow A_n \tag{14.23}$$

$$A_j \leftarrow A_{j-1} \tag{14.24}$$

$$A_1 \leftarrow M \tag{14.25}$$

M represents the concentration of the input to the A compartments, and N the concentration of the output. The countercurrent flow through the B compartments will involve:

$$P \leftarrow B_1 \tag{14.26}$$

$$B_{j-1} \leftarrow B_j \tag{14.27}$$

$$B_n \leftarrow Q \tag{14.28}$$

Q is the input to the low concentration side, and P is the output. The terminology for these procedures is given in Figure 14.4.

In contrast with countercurrent flow, concurrent flow involves the flow of the solution through the B compartments in the same direction as

through the A compartments. In Figure 14.4, concurrent flow through the B compartments would be from left to right. A simulation of concurrent flow would follow the same procedures as above, except that the sequence of Equations 14.26-14.28 would be reversed:

$$Q \leftarrow B_n \tag{14.29}$$

$$B_j \leftarrow B_{j-1} \tag{14.30}$$

$$B_1 \leftarrow P \tag{14.31}$$

Note that with concurrent flow, Q becomes the output and P the input for the B compartments.

Exercise 14-4: Program the model for countercurrent flow using a system of 20 pairs of A and B compartments ($n = 20$). Using subscripted variables will make your program much shorter than otherwise. This will allow you to write one FOR-NEXT loop to solve Equations 14.18-14.20 for all 20 pairs of compartments, and another loop to perform the updates with Equations 14.21-14.22. Then, a loop may be set up for the sequence involved with Equation 14.24, and finally another loop for Equation 14.27. Use constants of $a = 1.0$, and $p = 0.1$. Set $M = 100$ and $Q = 0$. For the Euler procedure let $\Delta t = 1$. Begin your simulation with A_1 through $A_n = 0$, and B_1 through $B_n = 0$. Allow your simulation to proceed for about 40 time intervals, and then plot concentration vs. compartment number for both A and B.

After you have produced the above output, modify your model to simulate concurrent flow, and run the simulation similarly. You can then compare efficiency of two flow types for lowering concentration of material in the A compartments.

14.5 A Model of Active Transport

A simple model for the active transport of some metabolite, B, into a cell may be developed from the following assumptions based on the diagram in Figure 14.5:

(1) Assume there are two compartments separated by a membrane with different permeabilities for substance B and a closely related compound C, with C having a higher permeability than B.

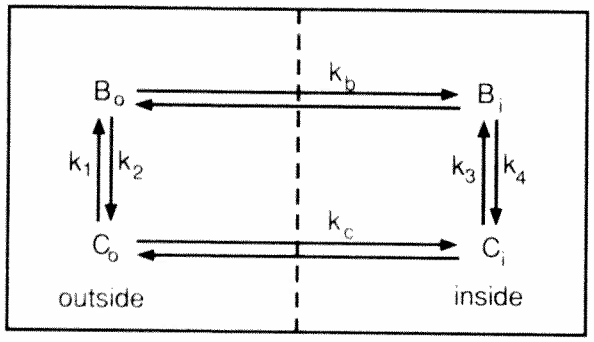

Figure 14.5. Diagram for a simple model of active transport. The terminology is explained in the text.

(2) Assume there is an enzyme on one side of the membrane which catalyzes the conversion of B to C. This might occur by a reaction such as:

$$B + W \rightleftharpoons C + X$$

where W is an activating molecule, such as ATP. In this reaction, the equilibrium lies far to the right, so that the equilibrium constant $K >> 1$ and $\Delta G_o << 0$.

(3) Assume there is another enzyme which catalyzes the conversion of C to B. This might occur as:

$$C + Y \rightleftharpoons B + Z$$

Again, the equilibrium is assumed to lie far to the right, and $\Delta G_o << 0$.

(4) Assume that concentrations of enzymes on each side of the membrane remain constant.

(5) Assume the two compartments have a unit volume and the separating membrane has a unit area. Following Equation 14.4, the rate of transport of B and C from inside the cell to the outside compartment due to diffusion would be described by these equations for the first stage of a two-stage Euler integration:

$$\Delta B_d = k_b (B_i - B_o) \Delta t \tag{14.32}$$

$$\Delta C_d = k_c (C_i - C_o) \Delta t \tag{14.33}$$

where k_b and k_c are diffusion rate constants, and B_i, B_o, C_i and C_o represent concentrations of the two compounds inside and outside of the cell.

(6) Assume that the enzymatic reactions follow first-order kinetics, which will be the case if the reactants other than B and C have constant concentrations, and if the enzymes are well below saturation by substrate. The reactions will alter the concentrations of B and C inside and outside the cell according to the following first-stage Euler equations:

$$\Delta B_i = (k_3 C_i - k_4 B_i) \Delta t \tag{14.34}$$

$$\Delta Ci = (k_4 B_i - k_3 C_i) \Delta t \tag{14.35}$$

$$\Delta B_o = (k_1 C_o - k_2 B_o) \Delta t \tag{24.36}$$

$$\Delta C_o = (k_2 B_o - k_1 C_o) \Delta t \tag{14.37}$$

where k_1, k_2, k_3, and k_4 are the rate constants for the reactions.

In the system based on the above assumptions, the concentration of B and C will be altered by diffusion and by the enzymatic reactions. The update expressions for the Euler integration of the equations will be

$$B_i \leftarrow B_i + \Delta B_i - \Delta B_d \tag{14.38}$$

$$B_o \leftarrow B_o + \Delta B_o + \Delta B_d \tag{14.39}$$

$$C_i \leftarrow C_i + \Delta C_i - \Delta C_d \tag{14.40}$$

$$C_o \leftarrow C_o + \Delta C_o + \Delta C_d \tag{14.41}$$

Exercise 14-5: Using the equations in Section 14.5, write and implement a program to simulate active transport of B against a diffusion gradient. Use the following rate constants, all with units of min^{-1}:

$$k_1 = 0.005 \qquad k_2 = 0.5 \qquad k_3 = 0.5$$
$$k_4 = 0.005 \qquad k_b = 0.001 \qquad k_c = 0.1$$

Begin your simulation with these initial values for concentration (mM l^{-1}):

$$B_o = 50 \qquad B_i = 50 \qquad C_o = 1 \qquad C_i = 1$$

Use a Δt value of 1.0 minute. Your output of the simulation should be a graph of the concentration of B_i and B_o against time. Allow the simulation to proceed to near steady-state.

14.6 Simple Approach to Active Transport

In the previous section we discussed a possible mechanism for active transport of a substance against a diffusion gradient. This resulted in a steady-state concentration gradient across the membrane. This same result could be obtained by simply employing different constants for the diffusion rates in each direction across the membrane.

In this case, rate of diffusion is described by a modification of Equation 14.3:

$$\frac{dQ_j}{dt} = k_1 \frac{Q_j}{V_j} - k_2 \frac{Q_i}{V_i} \tag{14.42}$$

where Q and V are defined as before, and k_1 is greater than k_2 if active transport is toward compartment i. At equilibrium the rates in each direction are equal, so that

$$k_1 \frac{Q_j}{V_j} = k_2 \frac{Q_i}{V_i} \tag{14.43}$$

and

$$\frac{k_1}{k_2} = \frac{Q_i V_j}{Q_j V_i} = \frac{C_i}{C_j} \tag{14.44}$$

Thus, the ratio of the two constants is equal to the equilibrium or steady-state ratio of the two concentrations, C_i and C_j.

Neither of the active transport processes described above account for mediated or facilitated transport processes. These are membrane transport processes, either active or passive, that show saturation-type kinetics because only a limited number of transport sites exist. In addition, they may show specificity for a particular chemical species being transported.

The distinction between simple diffusion and mediated-transport processes is seen in Figure 14.6. This shows graphically that the carrier or transport sites of the mediated-transport system become saturated at high concentrations of the diffusing substance, and that the rate does not exceed $T_{\max}$. This may be represented with a model equation of the Michaelis-Menten type:

$$T_c = T_{\max} \frac{C_i}{K_c + C_i} \tag{14.45}$$

where T_c is the rate of carrier-mediated diffusion, $T_{\max}$ is the maximum rate, C_i is the concentration of diffusing substance, and K_c is the half-saturation constant.

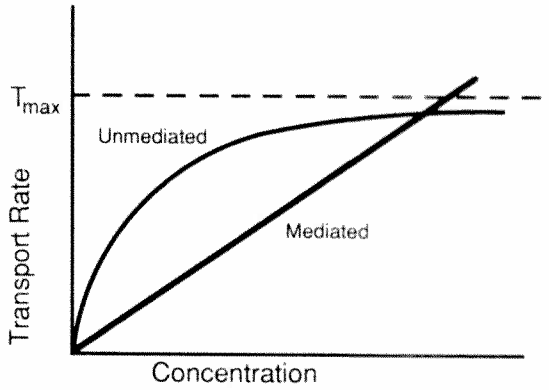

Figure 14.6. Graph showing general relationship between rates of transport and external concentration for mediated and unmediated (passive diffusion) transport processes. Based on a graph in Lehninger (1975).

Conclusion

As part of the coverage of compartmental models in physiology, this chapter has looked at simple models of diffusion. The modeling and simulation of diffusion can become quite complex; see Crank (1956) for example. The next chapter considers some different physiological models of fluid flow among compartments.